American Journal of Alzheimer's Disease & Other Dementias®
Volume 22 Number 6
December 2007/January 2008 474-488

10.1177/1533317507308779
http://ajadd.sagepub.com
hosted at
http://online.sagepub.com

Distinct MRI Atrophy Patterns in Autopsy-Proven Alzheimer's Disease and Frontotemporal Lobar Degeneration

G. D. Rabinovici, MD, W. W. Seeley, MD, E. J. Kim, MD, M. L. Gorno-Tempini, MD, PhD, K. Rascovsky, PhD, T. A. Pagliaro, BA, S. C. Allison, BS, C. Halabi, BS, J. H. Kramer, PsyD, J. K. Johnson, PhD, M. W. Weiner, MD, M. S. Forman, MD, PhD, J. Q. Trojanowski, MD, PhD, S. J. DeArmond, MD, PhD, B. L. Miller, MD, and H. J. Rosen, MD

To better define the anatomic distinctions between Alzheimer's disease (AD) and frontotemporal lobar degeneration (FTLD), we retrospectively applied voxel-based morphometry to the earliest magnetic resonance imaging scans of autopsy-proven AD (N = 11), FTLD (N = 18), and controls (N = 40). Compared with controls, AD patients showed gray matter reductions in posterior temporoparietal and occipital cortex; FTLD patients showed atrophy in medial prefrontal and medial temporal cortex, insula, hippocampus, and amygdala; and patients with both disorders showed atrophy in dorsolateral and orbital prefrontal cortex and lateral temporal cortex ($P_{FWE\text{-}corr} < .05$). Compared with FTLD, AD patients had decreased gray matter in posterior parietal and occipital cortex, whereas FTLD patients had selective atrophy in anterior cingulate, frontal insula, subcallosal gyrus, and striatum ($P < .001$, uncorrected). These findings suggest that AD and FTLD are anatomically distinct, with degeneration of a posterior parietal network in AD and degeneration of a paralimbic fronto-insular-striatal network in FTLD.

Keywords: Alzheimer's disease; frontotemporal lobar degeneration; autopsy; magnetic resonance imaging; voxel-based morphometry

From the Memory and Aging Center (GDR, WWS, EJK, MLG-T, KR, TAP, SCA, CH, JHK, JKJ, BLM, HJR) and Departments of Neurology (GDR, WWS, EJK, MLG-T, JHK, JKJ, BLM, HJR), Radiology (MWW), and Pathology (SJD), University of California, San Francisco, California; Magnetic Resonance Imaging Unit (MWW), San Francisco Veterans Affairs Hospital, San Francisco, California; Center for Neurodegenerative Disease Research (MSF, JQT) and Institute on Aging (MSF, JQT), Department of Pathology and Laboratory Medicine, University of Pennsylvania School of Medicine, Philadelphia, Pennsylvania.

This study was funded by the John Douglas French Alzheimer's Foundation; the Larry L. Hillblom Foundation; NIA grants P01-AG1972403, R01-AG022983, K08-AG027086-01, and K08-AG020760-01; ADRC grant P50-AG023501; and GCRC grant M01-RR00079.

The authors report no conflicts of interest.

Address correspondence to: Gil Rabinovici, MD, UCSF Memory & Aging Center, 350 Parnassus Ave, Suite 706, San Francisco, CA 94143; e-mail: grabinovici@memory.ucsf.edu.

Introduction

Alzheimer's disease (AD) and frontotemporal dementia (FTD) are the leading causes of early-onset dementia.[1,2] FTD describes a group of clinical syndromes, including 1 behavioral variant (bvFTD) and 2 language variants (semantic dementia [SD] and progressive nonfluent aphasia [PNFA]).[3] FTD can also be associated with motor neuron disease (FTD-MND).[4] FTD, clinically defined, most often reflects underlying frontotemporal lobar degeneration (FTLD) histopathology,[5] yet 15% to 30% of patients diagnosed with FTD antemortem show AD at autopsy.[6-8] The goal of this study was to identify magnetic resonance atrophy patterns that help distinguish pathologically proven FTLD and AD. For clarity, we use the term FTD to describe patients defined on clinical grounds and reserve the term FTLD to refer to

the group of related histopathologies commonly associated with FTD.

Structural imaging studies have identified signature atrophy patterns in AD and FTD. Compared with controls, patients with AD show greatest volume loss in hippocampus, medial temporal, and posterior temporoparietal cortices, whereas patients with FTD show atrophy throughout the frontal and anterior temporal lobes that varies depending on the specific FTD syndrome.[9-16] Although these atrophy patterns are somewhat distinct, there is considerable anatomic overlap between the 2 disorders. Volume loss in dorsolateral prefrontal cortex is common in AD (particularly in early-onset cases),[10-12,17-21] whereas hippocampal, medial temporal, and even parietal atrophy can occur in FTD.[19,21-25] Not surprisingly, visual assessment of medial temporal or frontal atrophy on magnetic resonance imaging (MRI) does not reliably discriminate between AD and FTD.[26]

Previous imaging studies that directly compared brain structure in AD and FTD have generally found greater frontal and anterior temporal atrophy in FTD and greater parietal atrophy in AD, with significant overlap in medial temporal structures.[13,19,21,22,24,27-30] These studies have a number of limitations. First, the majority of studies were based on region-of-interest analysis and, thus, did not explore potential differences across the whole brain.[22,24,27-30] Frontal lobe volumes were often measured as a single variable,[31,32] preventing detection of subregion-specific atrophy. Furthermore, most studies directly comparing AD and FTD stratified patients based on clinical rather than pathological diagnosis. Such studies are limited by potential circularity, because clinical syndromes that are influenced by anatomical focality are used to define regional differences between the 2 disorders. To our knowledge, no study to date has directly compared structural changes across the whole brain in pathologically proven AD and FTLD.

In this study, we used voxel-based morphometry (VBM)[33] to compare whole-brain atrophy patterns in autopsy-confirmed AD and FTLD. A better understanding of the anatomic distinctions between AD and FTLD could improve the diagnostic utility of MRI and focus the search for regional vulnerability mechanisms in each disease. A priori, we hypothesized that atrophy in a frontal paralimbic network, including anterior cingulate, frontal insula, and subcallosal gyrus, would discriminate FTLD from AD. Atrophy in these regions is common across clinical and pathologic FTD subtypes,[9,15,34] and the failure of social and emotional functions mediated by this network[35-37] leads to maladaptive behaviors that discriminate FTD from AD.[38-41] Furthermore, we hypothesized that atrophy in posterior parietal cortex would discriminate AD from FTLD. This region shows early functional and structural changes in AD[12,42,43] and mediates cognitive functions (eg, spatial navigation and visual construction) that are selectively impaired in AD compared with FTD.[44-46]

Methods

Patient Selection

We searched the University of California San Francisco Memory & Aging Center (UCSF MAC) database for all patients who underwent autopsy and met pathologic criteria for AD (NIA-Reagan)[47] or FTLD (McKhann).[5] Because our specific hypotheses about anatomic distinctions between the 2 disorders apply to FTLD pathologies that predominantly affect the frontal and anterior temporal cortex, we did not include patients with a pathologic diagnosis of corticobasal degeneration (CBD) (which often leads to asymmetric parietal as well as frontal atrophy) or progressive supranuclear palsy (PSP) (predominantly brainstem and subcortical atrophy).[48,49] In all the cases, patients or their surrogate decision makers provided a declaration of intent to undergo autopsy antemortem and next-of-kin provided consent to proceed with autopsy at the time of death.

We identified a total of 74 patients who had undergone autopsy between May 1999 and January 2007, 36 with AD and 38 with FTLD. Of these, 44 patients (20 AD and 24 FTLD) had a high-resolution MRI at our center during life. In the AD group, 3 patients were excluded because they did not meet NIA-Reagan criteria for high-likelihood AD, 3 were excluded because of mixed pathology (2 AD/PSP, 1 AD/CBD), 2 were excluded because of extensive white matter abnormalities on MRI (that confound image processing for VBM), and 1 patient was excluded because his autopsy tissue and report could not be reviewed. Patients with high-likelihood AD and comorbid Lewy bodies were included because of the high prevalence of Lewy bodies in pathologically confirmed AD, estimated at up to 60% when using modern immunohistochemistry.[50] In the FTLD group, 4 patients were excluded because of MRI motion artifact, 1 patient was excluded because of the presence of a right caudate infarct on imaging, and 1 patient was excluded because he was not considered demented at

Table 1. Clinical and Pathologic Diagnoses[a]

No.	Age at Death	Clinical Diagnosis	Pathologic Diagnosis	Comments
Alzheimer's disease				
1	62.6	AD possible	High probability AD	Infrequent limbic LBs
2	59.7	AD probable	High probability AD	Infrequent brainstem and limbic LBs
3	75.5	AD probable	High probability AD	Brainstem, limbic, and neocortical LBs
4	90.5	AD probable	High probability AD	Amyloid angiopathy
5	66.3	AD probable	High probability AD	Brainstem, limbic, and neocortical LBs; amyloid angiopathy
6	69.0	AD probable	High probability AD	Brainstem, limbic, and neocortical LBs; possible amyloid angiopathy
7	62.8	AD probable (PCA)	High probability AD	
8	73.2	AD/DLB probable	High probability AD	Neurofibrillary degeneration of brainstem nuclei
9	68.1	DLB probable	High probability AD	Brainstem, limbic, and neocortical LBs
10	61.9	bvFTD	High probability AD	
11	56.8	bvFTD	High probability AD	Neurofibrillary degeneration of brainstem nuclei
Frontotemporal lobar degeneration				
1	56.9	bvFTD	FTLD-DLDH	
2	74.4	bvFTD	Pick's (FTLD-T)	
3	72.1	bvFTD	Pick's (FTLD-T)	
4	68.3	bvFTD	Pick's (FTLD-T)	Moderate neuritic plaques; remote infarct frontal subcortical white matter
5	69.7	bvFTD	Pick's (FTLD-T)	Severe intracranial atherosclerosis with white matter ischemia
6	58.8	bvFTD	Pick's (FTLD-T)	
7	61.6	bvFTD	Pick's (FTLD-T)	
8	78.3	SD	Tauopathy NOS (FTLD-T)	Tau-positive grains and threads, mainly in hippocampus and temporal neocortex
9	53.5	bvFTD	FTLD-U/TDP-43	
10	76.8	SD	FTLD-U	TDP-43 stain not done
11	58.4	SD	FTLD-U/TDP-43	
12	73.5	SD	FTLD-U/TDP-43	
13	77.2	AD-MND vs PNFA-MND[b]	FTLD-U	Spinal cord not available; TDP-43 stain not done
14	63.5	FTD-MND	FTLD-U/TDP-43	Spinal cord not available
15	59.5	FTD-MND	FTLD-U/TDP-43	Spinal cord not available
16	53.3	FTD-MND	FTLD-MND (FTLD-U/TDP-43)	Remote infarcts left temporal pole and left orbital frontal cortex
17	59.3	FTD-MND	FTLD-MND (FTLD-U/TDP-43)	
18	53.1	PNFA-MND[c]	FTLD-MND (FTLD-U/TDP-43)	

Note: AD = Alzheimer's disease; FTLD = frontotemporal lobar degeneration; DLB = dementia with Lewy bodies; bvFTD = behavioral-variant frontotemporal dementia; MND = motor neuron disease; SD = semantic dementia; PNFA = progressive nonfluent aphasia; FTLD-DLDH = FTLD with dementia lacking distinctive histology; FTLD-T = FTLD with tau-positive inclusions; FTLD-U = FTLD with ubiquitin-positive/tau-negative inclusions; FTLD-U/TDP-43 = FTLD with ubiquitin and TDP-43 positive inclusions; FTLD-MND = FTLD that also meets pathologic criteria for motor neuron disease; NOS = not otherwise specified; LBs = Lewy bodies.

a. Age at death is shown in years. Clinical diagnosis refers to diagnosis at the time of MRI. Clinical diagnosis did not change by autopsy unless otherwise specified.

b. Diagnosis at autopsy was FTD-MND.

c. Diagnosis at autopsy was AD-MND versus PNFA-MND.

the time of death (this patient had amyotrophic lateral sclerosis but did not meet clinical research criteria for FTD). The final cohort consisted of 11 AD and 18 FTLD patients (Table 1). Thirteen autopsies were performed at the University of Pennsylvania, 12 at UCSF, 1 autopsy was shared by UCSF and the University of

Table 2. Group Characteristics[a]

	AD (N = 11)	FTLD (N = 18)	NC (N = 40)	*P*
Gender (M:F)	5:6	15:3	17:23	0.01[b]
Education (years)	16.5 ± 2.9	17.2 ± 2.2	17.4 ± 2.4[c]	NS
Age at MRI (years)	64.5 ± 9.7	62.5 ± 8.7	63.5 ± 5.8	NS
Onset to MRI (years)	6.0 ± 4.6	5.8 ± 4.2	N/A	NS
MRI to death (years)	3.4 ± 2.0	2.5 ± 1.7	N/A	NS
MMSE	19.9 ± 6.9	21.9 ± 8.2[c]	29.7 ± 0.5	< .001[d]
CDR—total	1.2 ± 0.5[c]	1.0 ± 0.6[c]	N/A	NS
CDR—sum of boxes	7.3 ± 2.6[c]	5.7 ± 3.2[c]	N/A	NS

Note: AD = Alzheimer's disease; FTLD = frontotemporal lobar degeneration; NC = normal control; MRI, magnetic resonance imaging; MMSE = Mini-Mental State Examination; CDR = Clinical Dementia Rating; N/A = not applicable; NS = not significant ($P > .05$).

a. Continuous variables are presented as means ± standard deviations.

b. Individual comparisons significant between FTLD and controls ($P < .001$) and between FTLD and AD ($P < .05$).

c. Data not available for all subjects.

d. Post hoc significant between AD and controls ($P < .001$) and between FTLD and controls ($P < .001$).

Pennsylvania, and 1 autopsy each was performed at the University of California at Irvine, Stanford University, and the University of Southern California.

All the patients had undergone at least 1 clinical evaluation at the MAC, which included a history and physical examination by a neurologist, a structured caregiver interview administered by a nurse, and a previously described battery of neuropsychologic tests.[46] Patients' functional statuses were measured using the Clinical Dementia Rating Scale (CDR).[51] Forty imaging controls were selected based on age matching from a pool of cognitively normal volunteers followed at the MAC. None of the controls had a history of neurologic or psychiatric illness. All the controls underwent a comprehensive clinical evaluation similar to the patient evaluations. None of the controls underwent autopsy.

Clinical diagnoses (including "normal control") were determined at a multidisciplinary conference. Standard research criteria were used for the diagnosis of AD (NINCDS-ADRDA)[52]; the FTD clinical syndromes bvFTD, SD, and PNFA (Neary)[3]; and dementia with Lewy bodies (DLB) (McKeith).[50,53] Clinical diagnosis at patients' first evaluation was blinded to imaging findings. In all the patients followed longitudinally, the diagnosis closest to the date of the MRI is presented, and longitudinal changes in diagnosis are also noted (Table 1). Onset of symptoms was determined retrospectively based on the estimated date of the first symptom, as identified by patients or caregivers and documented in medical records.

Patients and controls were well matched for age and education, although male gender was more common in FTLD than in AD or controls (Table 2). AD and FTLD patients were well matched for disease duration, time from MRI to autopsy, and dementia severity as measured by the Mini-Mental State Exam[54] and the CDR total and sum of box scores.

Image Acquisition and Analysis

MRI scans were performed on a 1.5-T Magnetom VISION system (Siemens Inc, Iselin, NJ) using a previously published protocol.[9] In patients with multiple MRIs, only the earliest MRI was included in the analysis. VBM[33] was performed using a previously described protocol[55] that includes creation of a study-specific template and custom tissue class prior probability maps.[56-58] This optimized protocol yields more biologically plausible results in neurodegenerative disease than the original VBM methods.[59] Gray matter voxel values were multiplied by the Jacobian determinants derived from spatial normalization to preserve the original volumes. Images were smoothed using a 12-mm full-width at half-maximum isotropic Gaussian kernel. Total intracranial volume (sum of gray matter, white matter, and CSF volumes derived from image segmentation) was entered into the design matrix as a global correction factor, and age and sex were entered as nuisance variables. Comparisons were made using the following contrasts: (1) AD < normal controls (NC), (2) FTLD < NC, (3) AD < FTLD, (4) FTLD < AD, (5) NC

< AD, and (6) NC < FTLD. To identify regions of gray matter loss that occur in both AD and FTLD compared with controls, we tested the conjunction null hypothesis when combining the contrasts AD < NC and FTLD < NC (conjunction analysis).[60] To allow broad visualization of the data, results were displayed on the study-specific template as t-maps thresholded at $P < .001$ (uncorrected for multiple comparisons). Voxels were considered significant at $P < .05$ after family-wise error (FWE) correction for multiple comparisons. All image processing and analyses were implemented in the SPM2 software package (http://www.fil.ion.ucl.ac.uk/spm).

Neuropathology

Twenty-six of 29 autopsies were performed at the University of Pennsylvania or at UCSF using a previously published protocol.[6] Autopsy reports from outside institutions were reviewed by a neurologist (GDR) to ensure adherence to a comparable protocol. At a minimum, all autopsies were required to include tissue sampling in regions relevant to the differential diagnosis of dementia based on published consensus criteria,[5,47,50] tissue staining with hematoxylin/eosin and thioflavin S or Bielschowsky silver staining, and immunohistochemistry using antibodies against Aβ, tau or hyperphosphorylated tau, α-synuclein, and ubiquitin. The pathologic diagnosis of AD was based on high likelihood by NIA-Reagan criteria[47] and FTLD on the diagnostic algorithm of the McKhann work group.[5] FTLD cases were divided into 3 subtypes based on distinct patterns of intracellular inclusions on immunohistochemical staining: (1) tau-positive inclusions with or without Pick bodies (FTLD-T); (2) tau-negative, ubiquitin-positive inclusions (FTLD-U, with or without associated motor neuron disease, designated FTLD-MND); and (3) tau-negative, ubiquitin-negative inclusions (dementia lacking distinctive histology, FTLD-DLDH).[5]

Statistical Analysis

Group differences in continuous variables were examined using 1-way analysis of variance (ANOVA) and Tukey's post hoc contrasts (for comparisons involving 3 groups) or 2-tailed independent sample *t*-tests (for comparisons involving 2 groups). Dichotomous variables were analyzed using χ^2 tests. Statistical analyses were implemented in SPSS 12.0 for Windows software (SPSS Inc, Chicago, IL).

The study was approved by the UCSF and University of Pennsylvania committees on human research.

Results

Clinicopathologic Correlations

Pathologic and clinical diagnoses are presented in Table 1. Four patients in the AD group had comorbid neocortical Lewy bodies, whereas 2 patients showed neurofibrillary degeneration of brainstem nuclei. Ten of 18 FTLD patients had FTLD-U, at times associated with FTLD-MND. While this study was in progress, the TAR DNA-binding protein TDP-43 was found to be the ubiquitinated protein associated with FTLD-U and FTLD-MND inclusions.[61] Eight of 10 FTLD-U/FTLD-MND cases included in this study were assessed with TDP-43 immunohistochemistry and all 8 cases showed TDP-43 immunoreactive intraneuronal inclusions. Six of 7 FTLD-T patients had Pick's disease, whereas 1 patient had a nonspecific tauopathy.

Two patients with a pathologic diagnosis of AD had a clinical diagnosis of bvFTD. One patient from the AD group had a clinical diagnosis of DLB and was found to have neocortical Lewy bodies. Another patient with a clinical diagnosis of mixed AD/DLB had neurofibrillary degeneration of brainstem nuclei, but no Lewy bodies on autopsy.

The majority of FTLD patients had bvFTD or FTD-MND clinically. All patients with a clinical diagnosis of MND had tau-negative, ubiquitin immunoreactive pathology. Three of 6 also met pathologic criteria for FTLD-MND (the spinal cord was not available for examination in the 3 patients who did not meet criteria). One patient with clinical MND had a diagnosis of "AD versus PNFA" at the time of his first MRI. The clinical diagnosis was changed to FTD-MND at a subsequent visit 16 months later. In contrast, 1 patient with FTLD-MND pathology had a diagnosis of PNFA-MND at first MRI, which was changed to "PNFA-MND versus AD-MND" at a later clinical evaluation. All 6 patients with Pick's disease presented clinically as bvFTD, as did the patient with DLDH. Three of 4 SD patients had FTLD-U whereas the other had a nonspecific tauopathy.

Voxel-Based Morphometry

AD <NC. Compared with controls, AD patients showed diffusely decreased cortical gray matter, most pronounced in posterior temporoparietal regions ($P < .001$, uncorrected for multiple comparisons; Figure 1A). Significant voxels were found bilaterally in inferior frontal, right superior frontal, and right posterior orbital

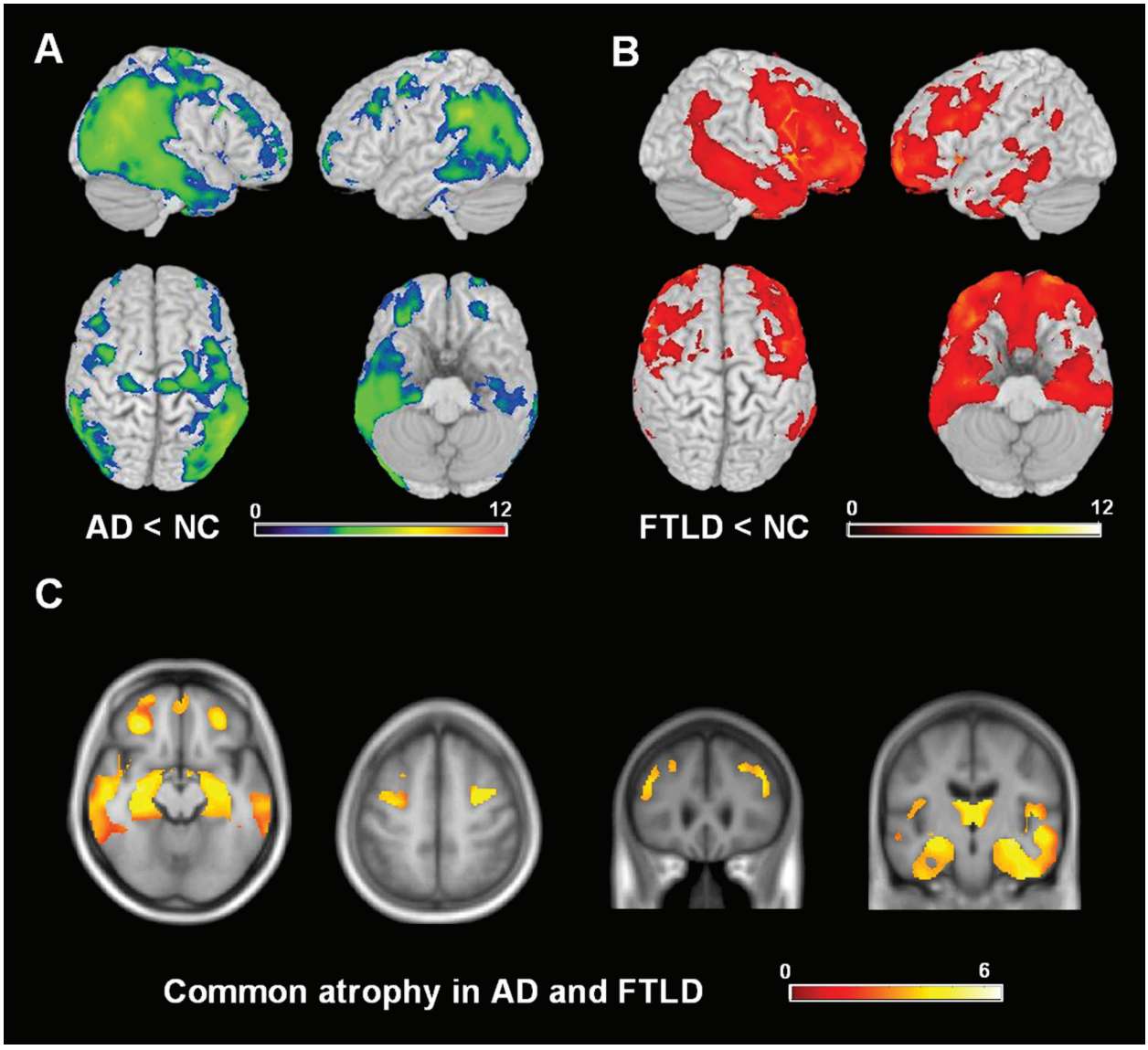

Figure 1. (A, B) Patterns of gray matter loss in autopsy-proven Alzheimer's disease (AD) (A) and frontotemporal lobar degeneration (FTLD) (B) compared with controls. *T* score maps are rendered on the Montreal Neurological Institute template brain. (C) Conjunction of contrasts shown in (A) and (B). *T* score maps are displayed on axial (from left, $z = -15$ and 52) and coronal (from left, $y = 28$ and -15) sections of the study-specific template brain in neurologic orientation. All results are presented at a threshold of $P < .001$ uncorrected. To highlight gray matter structures for display purposes, the findings are presented using the segmented gray matter image of the study-specific template as a region of interest.

gyrus; bilateral precentral gyrus; bilateral angular and supramarginal gyri; bilateral middle temporal gyrus and right superior temporal sulcus; bilateral middle occipital gyrus; and bilateral caudate head ($P_{FWE\text{-}corr} < .05$, Table 3). Posterior cingulate, precuneus, medial temporal cortex, hippocampus, and amygdala were atrophic bilaterally at $P < .001$ uncorrected, but did not survive multiple comparisons correction.

FTLD < NC. Compared with controls, FTLD patients demonstrated gray matter loss predominantly in the frontal and anterior temporal lobes, though atrophy did extend to posterior temporal and parietal cortex, particularly on the right ($P < .001$, uncorrected; Figure 1B). Following multiple comparisons correction, significant voxels were found bilaterally in dorsolateral prefrontal cortex, anterior

Table 3. Regions of Gray Matter Loss in AD and FTLD Compared With Cognitively Normal Controls[a]

Structure	BA	*x*	*y*	*z*	*T*	*P* (FWE-corr)
AD < NC						
L Superior frontal gyrus	6	−24	−9	51	5.86	0.01
R Inferior frontal gyrus	44	38	9	33	5.82	0.01
	44	41	20	29	5.44	0.03
L Inferior frontal gyrus	44	−38	10	27	6.77	0.00
R Posterior orbital gyrus	11	29	37	−11	5.82	0.01
R Precentral gyrus	6	27	−16	75	5.49	0.02
L Precentral gyrus	4	−31	−13	47	5.43	0.03
R Angular gyrus	39	58	−52	40	6.87	0.00
	39	47	−58	44	6.81	0.00
L Angular gyrus	40	−60	−45	33	7.05	0.00
R Supramarginal gyrus	40	43	−31	42	5.68	0.01
L Supramarginal gyrus	40	−54	−49	38	6.57	0.00
R Posterior middle temporal gyrus	37	48	−64	23	7.36	0.00
L Posterior middle temporal gyrus	37	−43	−55	16	6.98	0.00
R Superior temporal sulcus	21/22	55	−24	−7	6.10	0.00
R Middle occipital gyrus	19	42	−82	−3	5.66	0.01
L Middle occipital gyrus	19	−40	−80	1	5.32	0.01
R Caudate head	–	6	11	10	5.94	0.01
L Caudate head	–	−5	7	10	5.32	0.01
FTLD < NC						
L Superior frontal gyrus	10	−25	62	6	7.09	0.00
Cingulate sulcus/superior frontal gyrus (bilateral)	24/32	1	50	24	6.00	0.00
R Middle frontal gyrus	9	25	34	36	6.02	0.00
	46	28	48	20	5.84	0.01
	46	41	51	3	5.96	0.01
L Middle frontal gyrus	46	−26	13	47	5.76	0.01
L Middle frontal gyrus/pole	11	−25	63	0	6.89	0.00
R Inferior frontal gyrus, pars opercularis	44	50	11	18	8.04	0.00
L Inferior frontal gyrus, pars opercularis	44	−42	9	27	7.98	0.00
L Inferior frontal gyrus, pars triangularis	45	−54	26	25	6.29	0.00
L Inferior precentral sulcus	6/44	−52	3	38	6.27	0.00
R Anterior cingulate	24	8	25	20	5.90	0.01
L Anterior cingulate	24	−6	25	19	6.48	0.00
R Frontomarginal gyrus	11	24	74	−5	5.85	0.01
L Frontomarginal/medial orbital gyrus	11	−18	69	−19	5.24	0.05
Subcallosal gyrus (bilateral)	25	0	29	−10	6.06	0.00
R Medial orbital gyrus	11	22	67	−9	6.25	0.00
L Medial orbital gyrus	11	−22	65	−8	7.07	0.00
L Anterior orbital gyrus	11	−22	65	−8	7.07	0.00
L Lateral orbital gyrus	10/11	−39	55	−5	5.75	0.01
R Frontal insula	–	44	9	−5	7.65	0.00
L Frontal insula	–	−44	4	−4	6.29	0.00
R Mid insula	–	47	−4	−3	6.80	0.00
L Precentral gyrus	4	−34	−12	47	5.88	0.01
R Inferior temporal gyrus	20	45	−19	−44	7.01	0.00
R Fusiform gyrus	20	38	−16	−36	5.52	0.01
L Fusiform gyrus	20	−43	−21	−33	5.33	0.01
R Parahippocampal gyrus	36	26	−6	−30	5.89	0.01
L Parahippocampal gyrus	36	−27	−11	−34	5.37	0.01
	35	−36	−20	−41	5.89	0.01
L Isthmus/parahippocampal gyrus	27	−12	−33	−1	6.11	0.00
R Hippocampus	20	32	−20	−14	7.32	0.00
L Hippocampus	20	−28	−20	−14	6.38	0.00
R Amygdala	–	20	3	−21	5.85	0.01
L Amygdala	–	−20	1	−20	7.73	0.00

R Caudate head	–	9	16	7	11.00	0.00
L Caudate head	–	−7	13	8	11.63	0.00
L Putamen	–	−18	6	2	10.19	0.00
Conjunction (AD < NC) and (FTLD < NC)						
L Middle frontal gyrus	9	−31	−13	47	5.43	0.03
R Inferior frontal gyrus	44	38	9	33	5.82	0.01
	45	41	20	29	5.44	0.03
L Inferior frontal gyrus	44	−38	10	27	6.77	0.00
R Posterior orbital gyrus	47	29	37	−11	5.82	0.01
R Posterior superior temporal sulcus	21/22	55	−23	−8	6.12	0.00
R Caudate head	–	6	11	10	5.94	0.01
L Caudate head	–	−5	11	8	5.41	0.03

Note: AD = Alzheimer's disease; FTLD = frontotemporal lobar degeneration; NC = normal control; BA = Brodmann area; *T* = *T* score at given voxel; *P* (FWE-corr) = *P* value corrected via familywise error for multiple comparisons.
a. Coordinates of peak voxels are presented in millimeters in Montreal Neurological Institute stereotactic space.

cingulate, orbital frontal cortex, frontal poles, subcallosal gyrus, and frontal insula; left precentral gyrus; bilateral fusiform and parahippocampal gyri and right inferior temporal gyrus; bilateral hippocampus and amygdala; bilateral caudate head and left putamen ($P_{FWE\text{-}corr} < .05$, Table 3).

Conjunction of (AD < NC) and (FTLD < NC). Conjunction analysis revealed common regions of decreased gray matter in both AD and FTLD compared with controls in bilateral dorsolateral and orbital prefrontal cortex; bilateral angular and supramarginal gyri; throughout the temporal lobes; and in bilateral hippocampus, amygdala, and striatum ($P < .001$, uncorrected; Figure 1C). Following multiple comparisons correction, significant voxels were found in left middle frontal gyrus, right posterior orbital gyrus, and bilateral inferior frontal gyrus; right posterior superior temporal sulcus; and bilateral head of the caudate ($P_{FWE\text{-}corr} < .05$, Table 3).

AD < FTLD. Compared with FTLD patients, AD patients had decreased gray matter in the right precentral gyrus, left superior parietal lobule and supramarginal gyrus and bilateral angular gyrus, bilateral middle occipital gyrus and left intraoccipital sulcus ($P < .001$, uncorrected; Figure 2A, Table 4). None of these regions survived multiple comparisons correction.

FTLD < AD. Compared with AD patients, FTLD patients showed gray matter loss in left superior and inferior frontal gyrus, right frontal pole, and bilateral anterior cingulate; posterior orbital and subcallosal gyrus; anterior insula and striatum ($P < .001$, uncorrected; Figure 2A and B, Table 4). Only bilateral striatum was significant after multiple comparisons correction ($P_{FWE\text{-}corr} < .05$).

Other contrasts. The contrasts NC < FTLD and NC < AD did not yield significant results (at $P < .001$, uncorrected).

Discussion

In this study, we used VBM to compare gray matter loss in patients with pathology-proven AD and FTLD with cognitively normal controls and with each other. In general, our findings were consistent with previous imaging studies (largely based on clinical diagnosis)[9-14,16,24,28,38,62-64] and with the known gross and microscopic pathologic distribution of disease in AD[47,65] and FTLD.[66,67] We found that lateral parietal and occipital cortices are more atrophic in AD than in FTLD, whereas atrophy in a distinctive set of frontal paralimbic cortices (anterior cingulate, anterior insula, subcallosal gyrus) and the striatum differentiates FTLD from AD (Figure 2). In contrast, gray matter loss in dorsolateral prefrontal cortex and the medial temporal lobes (including hippocampus and amygdala) is found in both AD and FTLD compared with controls and does not help discriminate between the 2 disorders (Figure 1).

The majority of cortical areas specifically affected in FTLD (Figure 2) lie at transition zones between primitive allocortex and granular neocortex[68] and are robustly interconnected with each other and with subcortical regions prominently affected in FTLD, including the striatum and amygdala.[69] Converging evidence from lesion, functional neuroimaging, and neurophysiological studies has

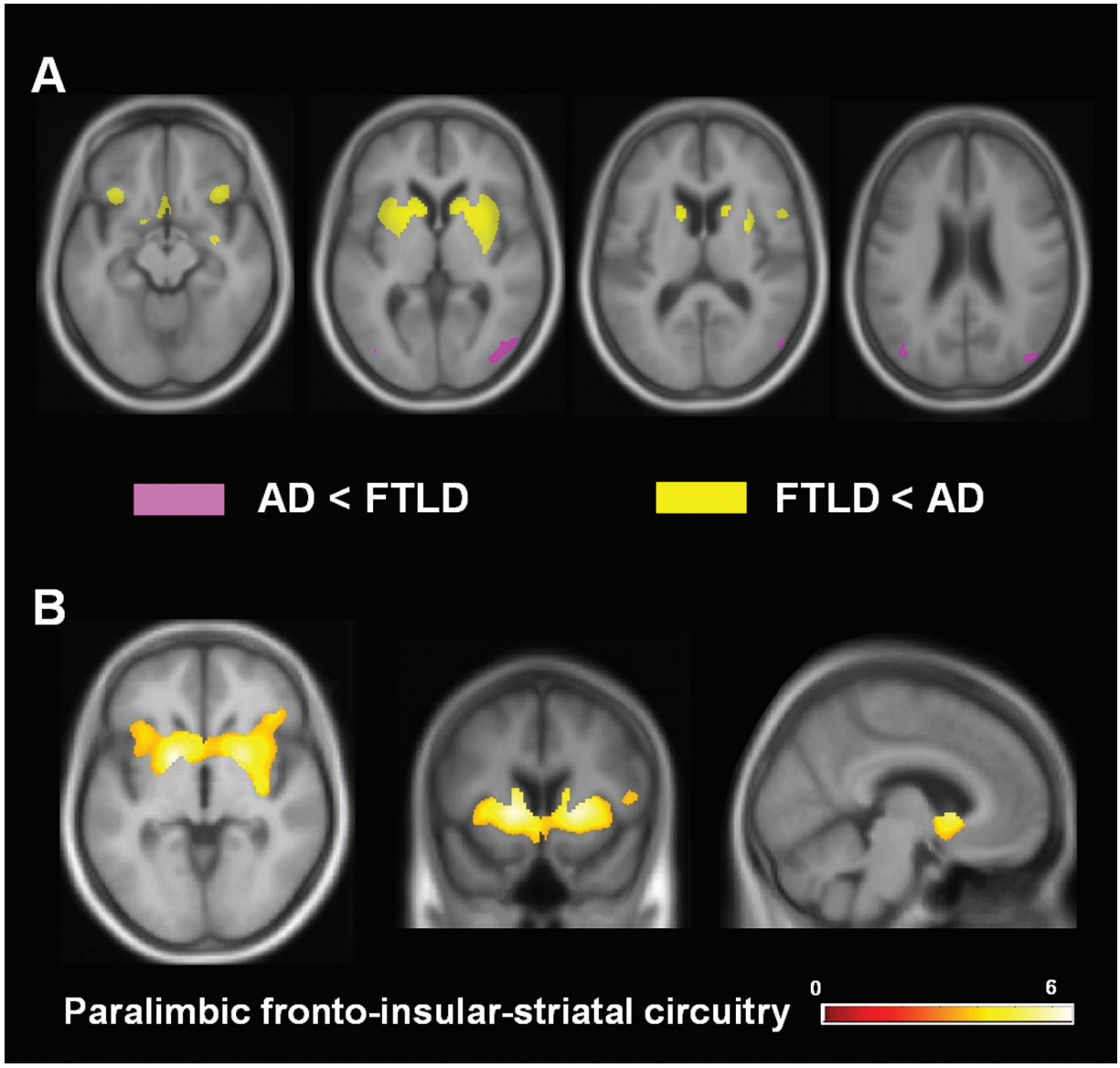

Figure 2. (A) Direct comparison of atrophy in pathology-proven frontotemporal lobar degeneration (FTLD) and Alzheimer's disease (AD). Regions of atrophy specific to AD (pink) and FTLD (yellow) are displayed on axial sections (from left, $z = -14$, 3, 11, and 24) of the study-specific template. (B) The FTLD < AD contrast highlights a fronto-insular-striatal paralimbic network. *T* score maps are displayed on axial ($z = -4$), coronal ($y = 11$), and sagittal ($x = -6$) sections of the study-specific template in neurologic orientation. All results are presented at a threshold of $P < .001$ uncorrected. For display purposes, the data are shown using the segmented gray matter image of the study-specific template as a region of interest.

demonstrated the importance of this anterior paralimbic circuit in mediating emotional and social function, decision making related to reward-punishment contingencies, and autonomic-interoceptive processing.[35,37,69-73] The unifying function of the network may be to grade the social, emotional, or motivational salience of internal and external stimuli to guide adaptive, context-specific behavior.[37] Failure of the FTLD paralimbic system can result in a host of maladaptive behaviors, many of which discriminate FTLD from AD, including disinhibition, apathy, obsessive-compulsive behaviors, failure to infer the mental state of others, and loss of empathy, satiety, disgust, and pain.[39-41,74] Cognitive tasks that engage the anterior paralimbic system are impaired in FTLD[75] and help distinguish FTLD and AD.[76] This network is further characterized by the

Table 4. Regions of Gray Matter Loss That Distinguish AD and FTLD[a]

Structure	BA	*x*	*y*	*z*	*T*
AD < FTLD					
R Precentral gyrus	6	27	−16	75	3.54
L Superior parietal lobule	7	−19	−50	46	3.67
L Supramarginal gyrus	40	−49	−58	60	3.77
R Intraparietal sulcus	7	37	−86	47	3.88
R Angular gyrus	39	36	−61	26	4.10
L Angular gyrus	39	−38	−54	28	4.76
L Intraoccipital sulcus	18/19	−26	−94	32	4.01
R Middle occipital gyrus	19	33	−74	17	3.92
	19	37	−76	−2	5.01
L Middle occipital gyrus	19	−39	−79	−2	4.10
FTLD < AD					
L Superior frontal gyrus (pole)	10	9	78	1	3.53
L Inferior frontal gyrus (pars opercularis)	44	54	12	10	3.58
L Anterior cingulate	24	−6	22	26	3.32
R Frontomarginal gyrus	11	18	77	0	4.37
R Posterior orbital gyrus	47	37	25	−9	4.44
L Posterior orbital gyrus	47	−35	22	11	4.14
Subcallosal gyrus (bilateral)	25	0	21	−12	3.41
R Frontal insula	–	33	20	−6	3.79
L Frontal insula	–	−33	20	−5	3.90
R Striatum	–	22	9	0	5.70[b]
L Striatum	–	−17	6	0	6.24[b]

Note: AD = Alzheimer's disease; FTLD = frontotemporal lobar degeneration; BA = Brodmann area; *T* = *T* score at given voxel.
a. Coordinates of peak voxels are presented in millimeters in Montreal Neurological Institute stereotactic space.
b. Voxels significant at *P* (FWE-corr) < .05.

presence of von Economo neurons, a group of large, bipolar projection neurons found only in great apes, humans, and selected whales and localized almost exclusively to anterior cingulate and frontal insular cortex.[77,78] von Economo neurons are selectively lost in FTLD compared with both AD and controls, providing a possible clue to the biological substrate of FTLD-selective regional vulnerability.[79]

Gray matter loss in posterior association cortices, including superior and inferior parietal lobules and visual association cortex, was greater in AD than in FTLD (Figure 2A). In AD, β-amyloid deposition, tissue hypometabolism, and cortical atrophy all converge in heteromodal parietal association cortex.[80] Metabolic and structural changes in posterior parietal cortex are apparent in early AD and even in presymptomatic apolipoprotein E4 carriers.[81] These regions are engaged in episodic memory retrieval[82] as well as in spatial and visual construction tasks that discriminate AD from FTLD.[45,46] Parietal association cortices are tightly interconnected with the medial temporal lobes,[83] and this connectivity is disrupted in AD.[84] Our inability to detect selective atrophy of medial parietal cortex (including posterior cingulate and precuneus), a critical component of the AD network, may reflect a lack of power because of the limited number of AD cases.

Atrophy in visual association cortex in AD compared with FTD has been previously reported[19] and may, in part, reflect the relatively young ages of our AD patients (mean age 64.5 years, 7/11 patients younger than 65 years at the time of MRI). Cortical atrophy in early-onset AD (symptom onset before 65 years) is more diffuse than in late-onset AD and can involve visual association areas.[85] Although the patients in our study were not all prospectively evaluated for the posterior cortical atrophy (PCA) syndrome, which is associated with greater occipital atrophy than "typical" AD,[86] review of medical records revealed that 1 patient was clinically diagnosed with PCA (Table 1) and 2 patients had early or disproportionate visuospatial or visual perceptual deficits consistent with PCA.

Our finding of selective precentral gyrus atrophy in AD is surprising, because structural, functional, and pathologic changes in AD typically spare primary motor and sensory cortex.[85,87,88] However, atrophy and pathologic involvement of primary motor cortex in AD have been previously reported,[89,90] and the robust significance of this finding in the AD < NC contrast (Table 3) makes it less likely to be spurious. Motor symptoms and signs are also more common in early-onset AD.[91,92] Although a different set of results may have been expected had we compared atrophy in FTLD with late-onset AD (which shows greater hippocampal atrophy and less cortical atrophy compared with early-onset AD),[85] age-matched patient groups provide more clinically applicable findings, because FTLD enters the differential diagnosis most commonly in patients with early-onset dementia.[1,2]

In addition to searching for patterns of atrophy that discriminate between AD and FTLD, we also sought to find regional atrophy common to both disorders. A conjunction analysis revealed that atrophy in dorsolateral prefrontal cortex occurs in both AD and FTLD compared with controls (Figure 1C), consistent with reports that executive dysfunction is found in both disorders and does not reliably distinguish between them.[45,46] Furthermore, hippocampus and amygdala atrophy was seen in both diseases (at

$P < .001$ uncorrected, these regions survived multiple comparisons correction only in the FTLD < NC contrast), consistent with previous reports of medial temporal atrophy in both AD and FTD.[22,24] Striatal atrophy was found when comparing both patient groups with controls, as well as in the FTLD < AD contrast. Although the validity of VBM findings in periventricular regions remains a concern because of the imperfect registration of anatomic structures near large image gradients,[59,93] our group has recently validated striatal VBM findings using manual region-of-interest tracing.[34]

Our study has a number of limitations. First, the retrospective study design introduces potential bias. For one, neuropathologists were not blinded to clinical data, including neuroimaging findings, at the time of autopsy. However, the application of a standardized pathologic evaluation that takes into account a broad differential diagnosis for degenerative dementia decreases the chance that clinical data may have biased the autopsy diagnosis. Any potential bias related to imaging analysis is mitigated by our use of VBM, which is an automated, objective, and unbiased tool for comparing gray matter volumes. It is also worth noting that all clinical diagnoses presented in this study were made prospectively while the patients were alive, and the initial clinical diagnosis (Table 1) was blinded to imaging results. Further studies are necessary to determine whether our group-level, retrospective findings can be applied to prospectively predict underlying pathology in individual patients.

As with many imaging studies based on autopsy-proven diagnosis, small group sizes limited our power to detect significant differences in gray matter volume, especially in the direct patient group comparisons. For this reason, few of the voxels in the direct contrasts between AD and FTLD survived FWE correction for multiple comparisons (Table 4). However, the patterns of atrophy detected in these contrasts at an uncorrected threshold ($P < .001$) matched well with our a priori hypotheses as outlined in the Introduction. Furthermore, the FWE criteria were originally designed for functional imaging studies and may be overly stringent for VBM.[94] For these reasons, we believe that the head-to-head AD versus FTLD findings reported here are meaningful and valid though most did not meet our most stringent statistical criterion.

The FTLD group defined for this study included a number of clinical FTD and pathological FTLD subtypes. The majority of patients in our analysis (16/18) presented clinically as either bvFTD or SD (Table 1). Although these disorders are clinically and anatomically distinct, both variants share similar behavioral features,[3,95] and anterior paralimbic atrophy is a common denominator in both disorders.[9] Inclusion of patients with MND may have decreased our sensitivity to detect atrophy, because FTLD patients with MND generally show more restricted gray matter loss than those without MND.[96] Our analysis also included comparable numbers of the FTLD-U (N = 10) and FTLD-T (N = 7) pathologic subtypes. Significant overlap exists in the clinical presentation and anatomic patterns associated with these histopathologies.[6,7,15,34] Because the clinician is likely to encounter the full spectrum of FTLD-associated clinical and pathological variants, our approach allowed us to identify regions affected across subtypes that may best differentiate FTLD from AD. Antemortem prediction of specific FTLD pathology will be critical for developing and testing disease-specific therapies and represents an important area for future investigation.

In summary, this study found distinct patterns of brain atrophy in AD and FTLD, with greater posterior parietal atrophy in AD and greater FTLD-associated atrophy in an anterior fronto-insular-striatal network. Bedside tasks that selectively engage these networks may be of great utility in differential diagnosis. Further studies are necessary to determine whether these findings can improve diagnostic accuracy when prospectively applied to MRI scans from individual patients. Finally, special attention to the unique anatomic and biologic properties of these networks may yield further clues to the pathogenesis of AD and FTLD.

Acknowledgments

The authors would like to thank Victoria Beckman, Clarissa Bush, Erin Clevenger, Danijela Pavlic, Mamta Sattavat, Terry Schuck, and Diana Truran for their invaluable technical and administrative support.

References

1. Barker WW, Luis CA, Kashuba A, et al. Relative frequencies of Alzheimer disease, Lewy body, vascular and frontotemporal dementia, and hippocampal sclerosis in the State of Florida Brain Bank. *Alzheimer Dis Assoc Disord*. 2002;16:203-212.
2. Ratnavalli E, Brayne C, Dawson K, Hodges JR. The prevalence of frontotemporal dementia. *Neurology*. 2002;58:1615-1621.

3. Neary D, Snowden JS, Gustafson L, et al. Frontotemporal lobar degeneration: a consensus on clinical diagnostic criteria. *Neurology*. 1998;51:1546-1554.
4. Lomen-Hoerth C, Anderson T, Miller B. The overlap of amyotrophic lateral sclerosis and frontotemporal dementia. *Neurology*. 2002;59:1077-1079.
5. McKhann GM, Albert MS, Grossman M, Miller B, Dickson D, Trojanowski JQ. Clinical and pathological diagnosis of frontotemporal dementia: report of the Work Group on Frontotemporal Dementia and Pick's Disease. *Arch Neurol*. 2001;58:1803-1809.
6. Forman MS, Farmer J, Johnson JK, et al. Frontotemporal dementia: clinicopathological correlations. *Ann Neurol*. 2006;59:952-962.
7. Kertesz A, McMonagle P, Blair M, Davidson W, Munoz DG. The evolution and pathology of frontotemporal dementia. *Brain*. 2005;128:1996-2005.
8. Knibb JA, Xuereb JH, Patterson K, Hodges JR. Clinical and pathological characterization of progressive aphasia. *Ann Neurol*. 2006;59:156-165.
9. Rosen HJ, Gorno-Tempini ML, Goldman WP, et al. Patterns of brain atrophy in frontotemporal dementia and semantic dementia. *Neurology*. 2002;58:198-208.
10. Ishii K, Kawachi T, Sasaki H, et al. Voxel-based morphometric comparison between early- and late-onset mild Alzheimer's disease and assessment of diagnostic performance of z score images. *AJNR Am J Neuroradiol*. 2005;26:333-340.
11. Baron JC, Chetelat G, Desgranges B, et al. In vivo mapping of gray matter loss with voxel-based morphometry in mild Alzheimer's disease. *Neuroimage*. 2001;14:298-309.
12. Frisoni GB, Testa C, Zorzan A, et al. Detection of grey matter loss in mild Alzheimer's disease with voxel based morphometry. *J Neurol Neurosurg Psychiatry*. 2002;73:657-664.
13. Boxer AL, Rankin KP, Miller BL, et al. Cinguloparietal atrophy distinguishes Alzheimer disease from semantic dementia. *Arch Neurol*. 2003;60:949-956.
14. Karas GB, Burton EJ, Rombouts SA, et al. A comprehensive study of gray matter loss in patients with Alzheimer's disease using optimized voxel-based morphometry. *Neuroimage*. 2003;18:895-907.
15. Whitwell JL, Josephs KA, Rossor MN, et al. Magnetic resonance imaging signatures of tissue pathology in frontotemporal dementia. *Arch Neurol*. 2005;62:1402-1408.
16. Gorno-Tempini ML, Dronkers NF, Rankin KP, et al. Cognition and anatomy in three variants of primary progressive aphasia. *Ann Neurol*. 2004;55:335-346.
17. Busatto GF, Garrido GE, Almeida OP, et al. A voxel-based morphometry study of temporal lobe gray matter reductions in Alzheimer's disease. *Neurobiol Aging*. 2003;24:221-231.
18. Kawachi T, Ishii K, Sakamoto S, et al. Comparison of the diagnostic performance of FDG-PET and VBM-MRI in very mild Alzheimer's disease. *Eur J Nucl Med Mol Imaging*. 2006;33:801-809.
19. Du AT, Schuff N, Kramer JH, et al. Different regional patterns of cortical thinning in Alzheimer's disease and frontotemporal dementia. *Brain*. 2007;130:1159-1166.
20. Singh V, Chertkow H, Lerch JP, Evans AC, Dorr AE, Kabani NJ. Spatial patterns of cortical thinning in mild cognitive impairment and Alzheimer's disease. *Brain*. 2006;129:2885-2893.
21. Grossman M, McMillan C, Moore P, et al. What's in a name: voxel-based morphometric analyses of MRI and naming difficulty in Alzheimer's disease, frontotemporal dementia and corticobasal degeneration. *Brain*. 2004;127:628-649.
22. Barnes J, Whitwell JL, Frost C, Josephs KA, Rossor M, Fox NC. Measurements of the amygdala and hippocampus in pathologically confirmed Alzheimer disease and frontotemporal lobar degeneration. *Arch Neurol*. 2006;63:1434-1439.
23. Galton CJ, Gomez-Anson B, Antoun N, et al. Temporal lobe rating scale: application to Alzheimer's disease and frontotemporal dementia. *J Neurol Neurosurg Psychiatry*. 2001;70:165-173.
24. Chan D, Fox NC, Scahill RI, et al. Patterns of temporal lobe atrophy in semantic dementia and Alzheimer's disease. *Ann Neurol*. 2001;49:433-442.
25. Whitwell JL, Jack CR Jr, Baker M, et al. Voxel-based morphometry in frontotemporal lobar degeneration with ubiquitin-positive inclusions with and without progranulin mutations. *Arch Neurol*. 2007;64:371-376.
26. Likeman M, Anderson VM, Stevens JM, et al. Visual assessment of atrophy on magnetic resonance imaging in the diagnosis of pathologically confirmed young-onset dementias. *Arch Neurol*. 2005;62:1410-1415.
27. Boccardi M, Pennanen C, Laakso MP, et al. Amygdaloid atrophy in frontotemporal dementia and Alzheimer's disease. *Neurosci Lett*. 2002;335:139-143.
28. Galton CJ, Patterson K, Graham K, et al. Differing patterns of temporal atrophy in Alzheimer's disease and semantic dementia. *Neurology*. 2001;56:216-225.
29. Whitwell JL, Sampson EL, Watt HC, Harvey RJ, Rossor MN, Fox NC. A volumetric magnetic resonance imaging study of the amygdala in frontotemporal lobar degeneration and Alzheimer's disease. *Dement Geriatr Cogn Disord*. 2005;20:238-244.
30. Barnes J, Godbolt AK, Frost C, et al. Atrophy rates of the cingulate gyrus and hippocampus in AD and FTLD. *Neurobiol Aging*. 2007;28:20-28.
31. Bocti C, Rockel C, Roy P, Gao F, Black SE. Topographical patterns of lobar atrophy in frontotemporal dementia and Alzheimer's disease. *Dement Geriatr Cogn Disord*. 2006;21:364-372.
32. Boccardi M, Laakso MP, Bresciani L, et al. The MRI pattern of frontal and temporal brain atrophy in frontotemporal dementia. *Neurobiol Aging*. 2003;24:95-103.
33. Ashburner J, Friston KJ. Voxel-based morphometry—the methods. *Neuroimage*. 2000;11:805-821.

34. Kim EJ, Rabinovici GD, Seeley WW, et al. Patterns of MRI atrophy in tau-positive and ubiquitin-positive frontotemporal lobar degeneration. *J Neurol Neurosurg Psychiatry*. In press.
35. Devinsky O, Morrell MJ, Vogt BA. Contributions of anterior cingulate cortex to behaviour. *Brain*. 1995;118(pt 1):279-306.
36. Rolls ET, Hornak J, Wade D, McGrath J. Emotion-related learning in patients with social and emotional changes associated with frontal lobe damage. *J Neurol Neurosurg Psychiatry*. 1994;57:1518-1524.
37. Seeley WW, Menon V, Schatzberg AF, et al. Dissociable intrinsic connectivity networks for salience processing and executive control. *J Neurosci*. 2007;27:2349-2356.
38. Boccardi M, Sabattoli F, Laakso MP, et al. Frontotemporal dementia as a neural system disease. *Neurobiol Aging*. 2005;26:37-44.
39. Bozeat S, Gregory CA, Ralph MA, Hodges JR. Which neuropsychiatric and behavioural features distinguish frontal and temporal variants of frontotemporal dementia from Alzheimer's disease? *J Neurol Neurosurg Psychiatry*. 2000;69:178-186.
40. Bathgate D, Snowden JS, Varma A, Blackshaw A, Neary D. Behaviour in frontotemporal dementia, Alzheimer's disease and vascular dementia. *Acta Neurol Scand*. 2001;103: 367-378.
41. Snowden JS, Bathgate D, Varma A, Blackshaw A, Gibbons ZC, Neary D. Distinct behavioural profiles in frontotemporal dementia and semantic dementia. *J Neurol Neurosurg Psychiatry*. 2001;70:323-332.
42. Minoshima S, Giordani B, Berent S, Frey KA, Foster NL, Kuhl DE. Metabolic reduction in the posterior cingulate cortex in very early Alzheimer's disease. *Ann Neurol*. 1997; 42:85-94.
43. Scahill RI, Schott JM, Stevens JM, Rossor MN, Fox NC. Mapping the evolution of regional atrophy in Alzheimer's disease: unbiased analysis of fluid-registered serial MRI. *Proc Natl Acad Sci U S A*. 2002;99:4703-4707.
44. Elfgren C, Brun A, Gustafson L, et al. Neuropsychological tests as discriminators between dementia of Alzheimer type and frontotemporal dementia. *Int J Geriatr Psychiatry*. 1994; 9:635-642.
45. Rascovsky K, Salmon DP, Ho GJ, et al. Cognitive profiles differ in autopsy-confirmed frontotemporal dementia and AD. *Neurology*. 2002;58:1801-1808.
46. Kramer JH, Jurik J, Sha SJ, et al. Distinctive neuropsychological patterns in frontotemporal dementia, semantic dementia, and Alzheimer disease. *Cogn Behav Neurol*. 2003;16:211-218.
47. Consensus Recommendations for the Postmortem Diagnosis of Alzheimer's Disease. The National Institute on Aging, and Reagan Institute Working Group on Diagnostic Criteria for the Neuropathological Assessment of Alzheimer's Disease. *Neurobiol Aging*. 1997;18:S1-S2.
48. Josephs KA, Whitwell JL, Dickson DW, et al. Voxel-based morphometry in autopsy proven PSP and CBD [published online ahead of print]. *Neurobiol Aging*. 2006; November 9.
49. Boxer AL, Geschwind MD, Belfor N, et al. Patterns of brain atrophy that differentiate corticobasal degeneration syndrome from progressive supranuclear palsy. *Arch Neurol*. 2006;63:81-86.
50. McKeith IG, Dickson DW, Lowe J, et al. Diagnosis and management of dementia with Lewy bodies: third report of the DLB Consortium. *Neurology*. 2005;65:1863-1872.
51. Morris JC. The Clinical Dementia Rating (CDR): current version and scoring rules. *Neurology*. 1993;43: 2412-2414.
52. McKhann G, Drachman D, Folstein M, Katzman R, Price D, Stadlan EM. Clinical diagnosis of Alzheimer's disease: report of the NINCDS-ADRDA Work Group under the auspices of Department of Health and Human Services Task Force on Alzheimer's disease. *Neurology*. 1984;34:939-944.
53. McKeith IG, Galasko D, Kosaka K, et al. Consensus guidelines for the clinical and pathologic diagnosis of dementia with Lewy bodies (DLB): report of the Consortium on DLB International Workshop. *Neurology*. 1996;47:1113-1124.
54. Folstein MF, Folstein SE, McHugh PR. "Mini-mental state." A practical method for grading the mental state of patients for the clinician. *J Psychiat Res*. 1975; 12:189-198.
55. Rosen HJ, Allison SC, Schauer GF, Gorno-Tempini ML, Weiner MW, Miller BL. Neuroanatomical correlates of behavioural disorders in dementia. *Brain*. 2005;128: 2612-2625.
56. Good CD, Johnsrude I, Ashburner J, Henson RN, Friston KJ, Frackowiak RS. Cerebral asymmetry and the effects of sex and handedness on brain structure: a voxel-based morphometric analysis of 465 normal adult human brains. *Neuroimage*. 2001;14:685-700.
57. Good CD, Johnsrude IS, Ashburner J, Henson RN, Friston KJ, Frackowiak RS. A voxel-based morphometric study of ageing in 465 normal adult human brains. *Neuroimage*. 2001;14:21-36.
58. Testa C, Laakso MP, Sabattoli F, et al. A comparison between the accuracy of voxel-based morphometry and hippocampal volumetry in Alzheimer's disease. *J Magn Reson Imaging*. 2004;19:274-282.
59. Senjem ML, Gunter JL, Shiung MM, Petersen RC, Jack CR Jr. Comparison of different methodological implementations of voxel-based morphometry in neurodegenerative disease. *Neuroimage*. 2005;26:600-608.
60. Nichols T, Brett M, Andersson J, Wager T, Poline JB. Valid conjunction inference with the minimum statistic. *Neuroimage*. 2005;25:653-660.
61. Neumann M, Sampathu DM, Kwong LK, et al. Ubiquitinated TDP-43 in frontotemporal lobar degeneration and amyotrophic lateral sclerosis. *Science*. 2006; 314:130-133.

62. Mummery C, Patterson K, Price C, Ashburner J, Frackowiak R, Hodges J. A voxel-based morphometry study of semantic dementia: relationship between temporal lobe atrophy and semantic memory. *Ann Neurol*. 2000;47:36-45.
63. Frisoni GB, Beltramello A, Geroldi C, Weiss C, Bianchetti A, Trabucchi M. Brain atrophy in frontotemporal dementia. *J Neurol Neurosurg Psychiatry*. 1996;61:157-165.
64. Fukui T, Kertesz A. Volumetric study of lobar atrophy in Pick complex and Alzheimer's disease. *J Neurol Sci*. 2000;174:111-121.
65. Najlerahim A, Bowen DM. Regional weight loss of the cerebral cortex and some subcortical nuclei in senile dementia of the Alzheimer type. *Acta Neuropathol (Berl)*. 1988;75:509-512.
66. Broe M, Hodges JR, Schofield E, Shepherd CE, Kril JJ, Halliday GM. Staging disease severity in pathologically confirmed cases of frontotemporal dementia. *Neurology*. 2003;60:1005-1011.
67. Brun A, Gustafson L. Limbic lobe involvement in presenile dementia. *Arch Psychiatr Nervenkr*. 1978;226:79-93.
68. Mesulam MM. From sensation to cognition. *Brain*. 1998;121(pt 6):1013-1052.
69. Ongur D, Price JL. The organization of networks within the orbital and medial prefrontal cortex of rats, monkeys and humans. *Cereb Cortex*. 2000;10:206-219.
70. Damasio H, Grabowski T, Frank R, Galaburda AM, Damasio AR. The return of Phineas Gage: clues about the brain from the skull of a famous patient. *Science*. 1994;264:1102-1105.
71. Rolls ET. The functions of the orbitofrontal cortex. *Brain Cogn*. 2004;55:11-29.
72. Critchley HD. Neural mechanisms of autonomic, affective, and cognitive integration. *J Comp Neurol*. 2005; 493:154-166.
73. Augustine JR. Circuitry and functional aspects of the insular lobe in primates including humans. *Brain Res Brain Res Rev*. 1996;22:229-244.
74. Scherder EJ, Sergeant JA, Swaab DF. Pain processing in dementia and its relation to neuropathology. *Lancet Neurol*. 2003;2:677-686.
75. Rahman S, Robbins TW, Sahakian BJ. Comparative cognitive neuropsychological studies of frontal lobe function: implications for therapeutic strategies in frontal variant frontotemporal dementia. *Dement Geriatr Cogn Disord*. 1999;10(suppl 1):15-28.
76. Gregory C, Lough S, Stone V, et al. Theory of mind in patients with frontal variant frontotemporal dementia and Alzheimer's disease: theoretical and practical implications. *Brain*. 2002;125:752-764.
77. Nimchinsky EA, Gilissen E, Allman JM, Perl DP, Erwin JM, Hof PR. A neuronal morphologic type unique to humans and great apes. *Proc Natl Acad Sci U S A*. 1999; 96:5268-5273.
78. von Economo C. Eine neue Art Spezialzellen des Lobus cinguli und Lobus insulae. Z *Ges Neurol Psychiatr*. 1926;100:706-712.
79. Seeley WW, Carlin DA, Allman JM, et al. Early frontotemporal dementia targets neurons unique to apes and humans. *Ann Neurol*. 2006;60:660-667.
80. Buckner RL, Snyder AZ, Shannon BJ, et al. Molecular, structural, and functional characterization of Alzheimer's disease: evidence for a relationship between default activity, amyloid, and memory. *J Neurosci*. 2005;25: 7709-7717.
81. Reiman EM, Caselli RJ, Yun LS, et al. Preclinical evidence of Alzheimer's disease in persons homozygous for the epsilon 4 allele for apolipoprotein E. *New Engl J Med*. 1996;334:752-758.
82. Shannon BJ, Buckner RL. Functional-anatomic correlates of memory retrieval that suggest nontraditional processing roles for multiple distinct regions within posterior parietal cortex. *J Neurosci*. 2004;24:10084-10092.
83. Kobayashi Y, Amaral DG. Macaque monkey retrosplenial cortex: II. Cortical afferents. *J Comp Neurol*. 2003; 466:48-79.
84. Greicius MD, Srivastava G, Reiss AL, Menon V. Default-mode network activity distinguishes Alzheimer's disease from healthy aging: evidence from functional MRI. *Proc Natl Acad Sci U S A*. 2004;101:4637-4642.
85. Frisoni GB, Pievani M, Testa C, et al. The topography of grey matter involvement in early and late onset Alzheimer's disease. *Brain*. 2007;130:720-730.
86. Whitwell JL, Jack CR Jr, Kantarci K, et al. Imaging correlates of posterior cortical atrophy. *Neurobiol Aging*. 2007;28:1051-1061.
87. Arnold SE, Hyman BT, Flory J, Damasio AR, Van Hoesen GW. The topographical and neuroanatomical distribution of neurofibrillary tangles and neuritic plaques in the cerebral cortex of patients in Alzheimer's disease. *Cereb Cortex*. 1991;1:103-116.
88. Edison P, Archer HA, Hinz R, et al. Amyloid, hypometabolism, and cognition in Alzheimer disease. An [11C]PIB and [18F]FDG PET study. *Neurology*. 2007;68:501-508.
89. Busatto GF, Garrido GE, Almeida OP, et al. A voxel-based morphometry study of temporal lobe gray matter reductions in Alzheimer's disease. *Neurobiol Aging*. 2003;24:221-231.
90. Suva D, Favre I, Kraftsik R, Esteban M, Lobrinus A, Miklossy J. Primary motor cortex involvement in Alzheimer disease. *J Neuropathol Exp Neurol*. 1999;58:1125-1134.
91. von Gunten A, Bouras C, Kovari E, Giannakopoulos P, Hof PR. Neural substrates of cognitive and behavioral deficits in atypical Alzheimer's disease. *Brain Res Rev*. 2006;51:176-211.
92. Caviness JN. Myoclonus and neurodegenerative disease—what's in a name? *Parkinsonism Relat Disord*. 2003;9: 185-192.

93. Bookstein FL. "Voxel-based morphometry" should not be used with imperfectly registered images. *Neuroimage*. 2001;14:1454-1462.
94. Whitwell JL, Jack CR Jr. Comparisons between Alzheimer disease, frontotemporal lobar degeneration, and normal aging with brain mapping. *Top Magn Reson Imaging*. 2005;16:409-425.
95. Rosen HJ, Allison SC, Ogar JM, et al. Behavioral features in semantic dementia vs other forms of progressive aphasias. *Neurology*. 2006;67:1752-1756.
96. Whitwell JL, Jack CR Jr, Senjem ML, Josephs KA. Patterns of atrophy in pathologically confirmed FTLD with and without motor neuron degeneration. *Neurology*. 2006; 66:102-104.